

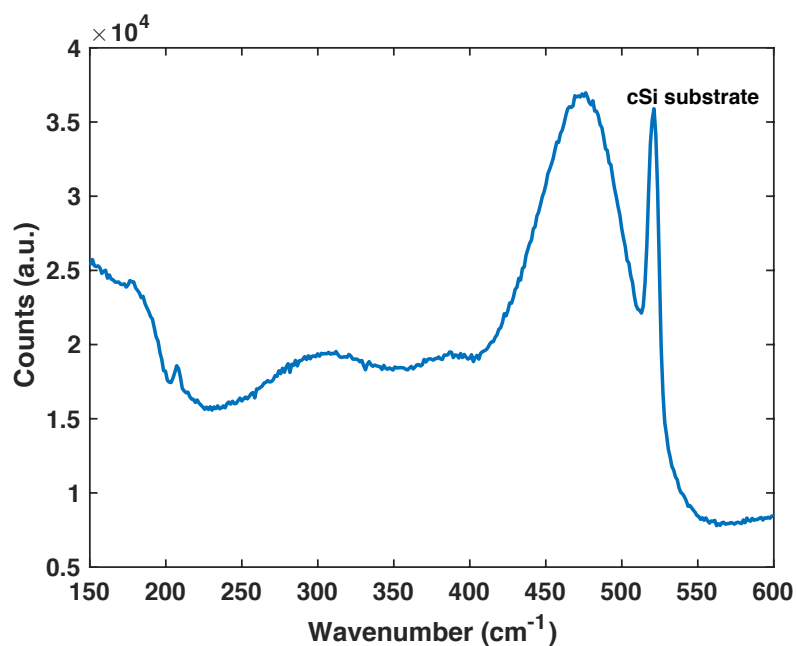
In the format provided by the authors and unedited.

**Photo-excited Hot Carrier Dynamics in Hydrogenated Amorphous Silicon Imaged
by 4D Electron Microscopy**

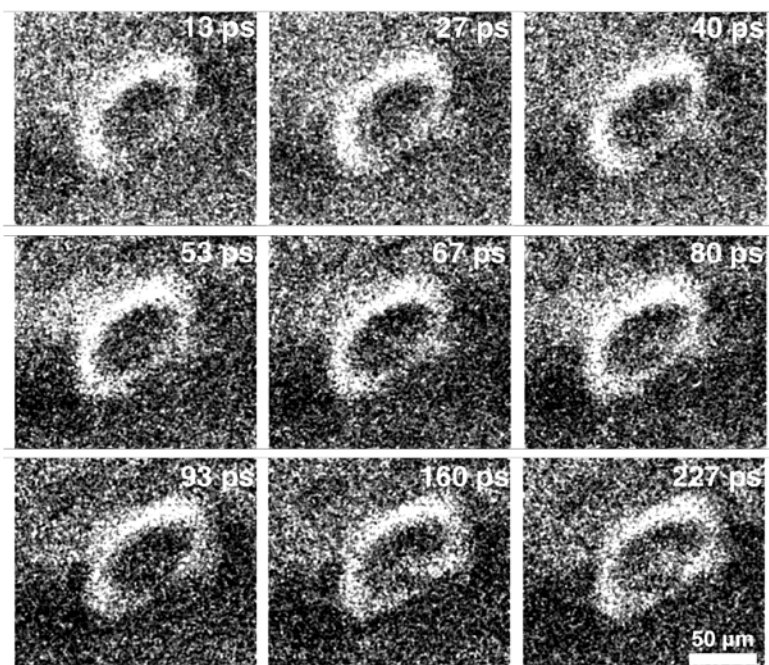
Bolin Liao, Ebrahim Najafi, Heng Li, Austin J. Minnich* and Ahmed H. Zewail†

* To whom correspondence should be addressed. Email: aminnich@caltech.edu

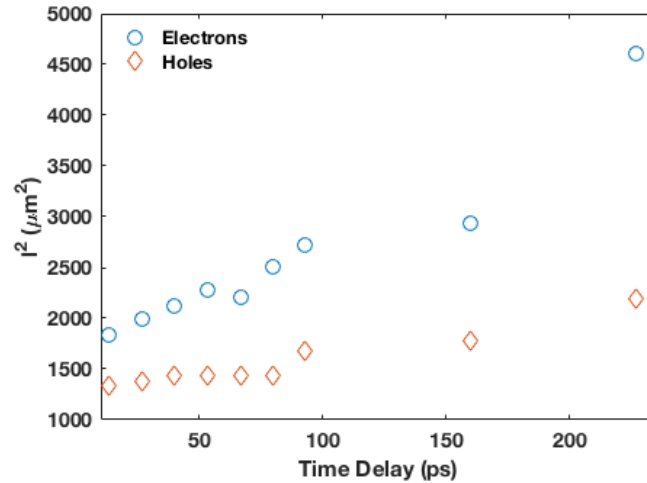
† Deceased



Supplementary Figure 1. Raman Characterization of the Sample. The Raman spectrum of the sample shows the wide “optical peak” of the amorphous silicon thin film at 475 cm⁻¹ (see Beeman et al.¹) and the narrow peak of the crystalline silicon substrate at 520 cm⁻¹.



Supplementary Figure 2. SUEM Images Taken at a Higher Pump Fluence. The data is measured with a pump fluence of $\sim 67 \mu\text{J}/\text{cm}^2$ (repetition rate at 5 MHz). The feature is significantly larger than that with the lower fluence as reported in the main text. This is because higher density of electrons and holes are excited above the detection threshold of the SUEM.



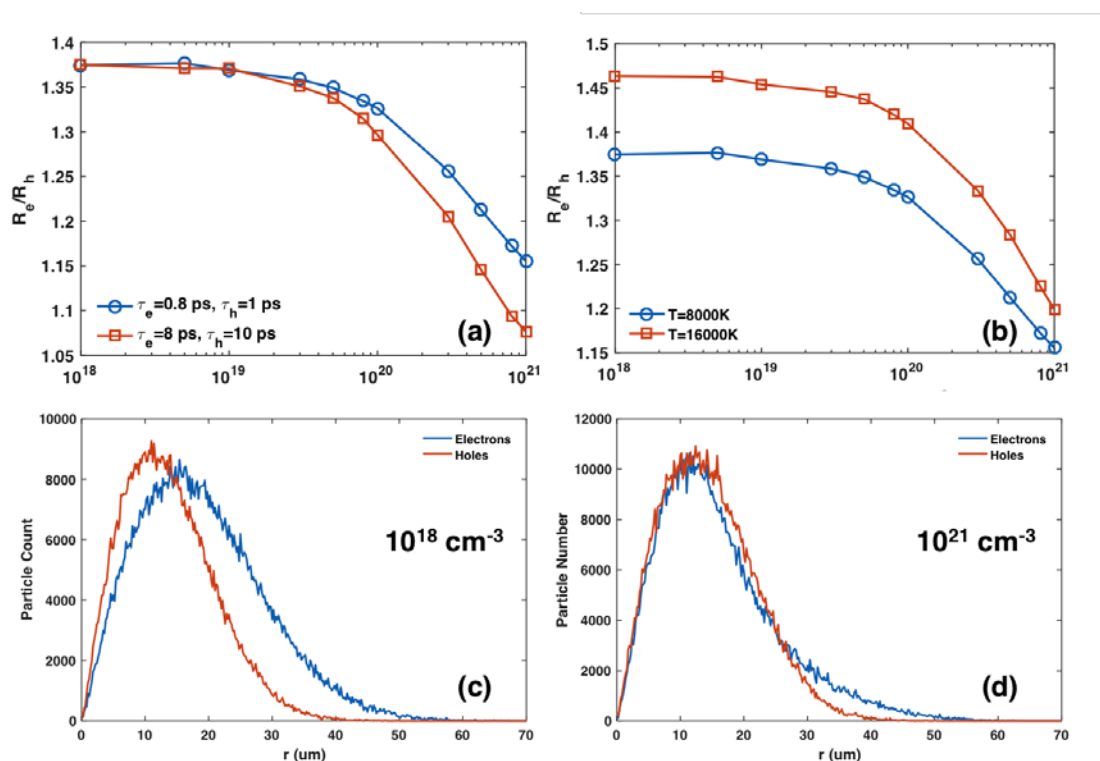
Supplementary Figure 3. Fast diffusion of electrons and holes at the higher pump fluence. The squared radii of the electron and hole distributions with the higher pump fluence ($67 \mu\text{J}/\text{cm}^2$) are shown as a function of time delay. In comparison to the data at the lower fluence reported in the main text, the time dependence here is closer to be linear, than quadratic, whereas the average speed of expansion is similar.

Supplementary Note 1: More discussion of the Monte Carlo simulation

In this Note, we provide more discussions of the Monte Carlo simulation, especially on the effect of various parameters in the simulation on the observed hot carrier dynamics. Intuitively speaking, the spontaneous electron-hole separation is controlled by two opposing forces: one that tends to drive electrons and holes apart, in this case the difference between the mobilities of electrons and holes and the initial high temperature; the other one that tends to hold electrons and holes together through Coulombic interaction, here characterised by the dielectric relaxation time, which is further controlled by the electrical conductivity. Another factor is the excited carrier concentration, which effectively controls the strength of the Coulombic interaction, because given the same spatial profiles of electrons and holes, higher carrier concentration leads to stronger electric field. This was also discussed by Ritter et al.² in their seminal study of a-Si:H. In other words, the electron-hole separation should always happen in principle as long as the mobilities of electrons and holes are different; but the extent of the separation is controlled by the initial velocities of electrons and holes (here controlled by the temperature), the electrical conductivity and the photoexcited carrier concentration. In the case presented here, the extent of separation is significant because of 1) large differences in the mobilities of electrons and holes; 2) the initial high temperature; 3) the low electrical conductivity and 4) the low concentration of photoexcited carriers.

To quantify the effect of each of these parameters, we use the ratio between the average widths of electron and hole distributions to characterise the extent of the charge separation, and study how the parameters affect the ratio using the Monte Carlo

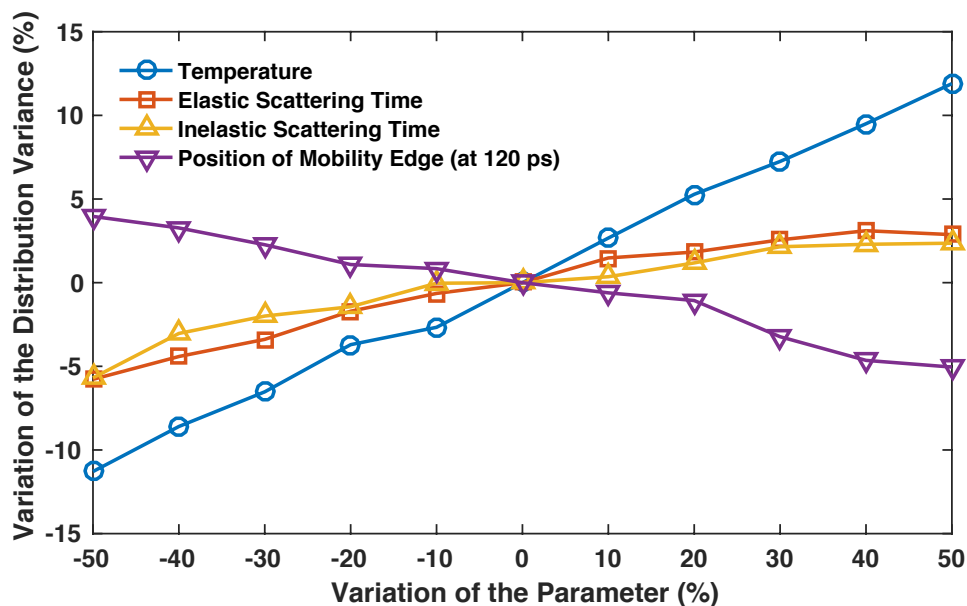
simulation. Shown in Supplementary Fig. 4 (a) is how the ratio at 40 ps after the photoexcitation is affected by the concentration of photocarriers and by the elastic scattering time of electrons and holes. All the other parameters are kept the same as reported in the main text. It is clearly seen from the simulation that, as the carrier concentration increases, the charge separation is suppressed, in agreement with the conclusion of Ritter et al.². Also when the elastic scattering time is increased, the charge separation becomes less significant. This is consistent with the fact that a longer scattering time corresponds to a higher electrical conductivity, and thus a shorter dielectric relaxation time. In Supplementary Fig. 4(b) we examine the effect of the initial temperature of electrons and holes. If this value is increased to 16000K, the charge separation is significantly enhanced, due to a stronger driving force to separate electrons and holes by diffusion. To illustrate the difference between charge-separation and ambipolar diffusion, the radial distribution functions of electrons and holes when the carrier concentration is 10^{18} cm^{-3} and 10^{21} cm^{-3} are shown and compared in Supplementary Fig. 4(c)(d). When the carrier concentration is high, the Coulombic interaction is strong enough to bind electrons and holes together, and the electron and hole distributions essentially overlap in space, as shown in Supplementary Fig. 4(d).



Supplementary Figure 4. Effects of the transport parameters on spontaneous charge separation. All results here are obtained at 40 ps after photoexcitation using Monte Carlo simulation. (a) The effect of carrier concentration and the elastic scattering time, while all other parameters are kept the same as reported in the main text. (b) The effect of carrier concentration and the initial temperature. The radial distribution functions of electrons and holes at carrier concentrations of 10^{18} cm $^{-3}$ and 10^{21} cm $^{-3}$ are shown in (c) and (d) respectively. The carrier concentration is controlled by varying how many electrons and holes are “represented” by one particle in the Monte Carlo simulation.

We further examine the sensitivity of the parameters used in the Monte Carlo simulation. We do this by calculating the change of the spatial variance of the electron/hole distribution after photoexcitation due to a variation of a certain parameter within $\pm 50\%$ of its optimal value. The results are shown in Supplementary Fig. 5, where the variance of the spatial distribution of electrons is calculated at 40 ps after photoexcitation when changing the initial temperature, elastic scattering time and inelastic scattering time of electrons by $\pm 50\%$, and at 120 ps after photoexcitation when changing the position of the mobility edge of electrons by $\pm 50\%$. It is seen from the plot

that the initial temperature is the most sensitive parameter that controls the early dynamics of electrons, and the position of the mobility edge mainly affects the trapping dynamics at longer delay times. Because we use the same set of parameters to fit experimental data at multiple delay times, the actual parametric sensitivity is better than that shown here in Supplementary Fig. 5, calculated only at a single delay time.



Supplementary Figure 5. The sensitivity of parameters used in the Monte Carlo simulation. For temperature, elastic scattering time and inelastic scattering time, the variance of the spatial distribution of electrons is calculated at 40 ps after photoexcitation; for the position of mobility edge, the variance of the spatial distribution of electrons is calculated at 120 ps after photoexcitation.

Supplementary Note 2: More discussion of the fast diffusion

There is a possibility that the observed initial fast diffusion is an artifact due to spatially-non-uniform recombination, which will reduce the electron concentration in the inner part of the disc but not in the outer part where there are no holes to recombine with. This will shift the peak electron concentration and give an artificially high diffusion rate. In the main text we interpret the decay of the image intensity shown in Fig. 3b as the charge trapping process into deep in-gap defect states, instead of recombination, for two reasons: 1) we observed a slightly faster decay of the intensity of the ring region than the center region. If this decay were due to charge recombination, then the intensity of the center region should decay much faster than the ring region, due to more overlap of electrons and holes in the center region as pointed out by the reviewer. 2) in our experiment the excited carrier concentration ($\sim 10^{18} \text{ cm}^{-3}$) is relatively low, and based on previous extensive optical studies of aSi:H (for example, ref. 11 in the main text and the references therein), in this regime carrier trapping is a much faster process than recombination. Since our measurement cannot directly distinguish the trapping and the recombination processes, we also estimate here how the measured diffusivity would be impacted if the decay shown in Fig. 3b were indeed due to recombination. The time scale of the decay shown in Fig. 3b is $\sim 1 \text{ ns}$, much longer than the time scale of the fast diffusion ($\sim 100 \text{ ps}$). Therefore, the decay of the image intensity in the first 100ps is roughly $1 - \exp(-0.1) \approx 9.5\%$. If this decay were caused by recombination, then the center region would decay faster than the outer region, effectively broadening the charge distribution, and leading to an overestimated diffusivity, which is the concern of the reviewer. To give a simple estimation, we consider a Gaussian distribution with width σ , and in the

extreme case, we assume the 9.5% decay only happens within the central region of $[-\sigma, \sigma]$. Then the effective width (variance) of the new distribution can be calculated to be 1.024σ . Because the diffusivity is proportional to the square of the effective width, it is overestimated by $\sim 5\%$ in this case. So this estimation indicates that the extracted diffusivity from our measurement would not be affected significantly even if recombination played a role in our experiment.

References

1. Beeman, D., Tsu, R. & Thorpe, M. Structural information from the Raman spectrum of amorphous silicon. *Phys. Rev. B* **32**, 874–878 (1985).
2. Ritter, D., Zeldov, E. & Weiser, K. Ambipolar transport in amorphous semiconductors in the lifetime and relaxation-time regimes investigated by the steady-state photocarrier grating technique. *Phys. Rev. B* **38**, 8296–8304 (1988).